Published in final edited form as:
Virology. 2014 September ; 0: 134–145. doi:10.1016/j.virol.2014.06.021.

Recombinant myxoma virus lacking all poxvirus ankyrin-repeat proteins stimulates multiple cellular anti-viral pathways and exhibits a severe decrease in virulence

Stephanie A. Lamb, **Masmudur M. Rahman**, and **Grant McFadden**
Dept of Molecular Genetics and Microbiology, College of Medicine, University of Florida, 1600 SW Archer Road, Gainesville, FL 32610, USA

Abstract

Although the production of single gene knockout viruses is a useful strategy to study viral gene functions, the redundancy of many host interactive genes within a complex viral genome can obscure their collective functions. In this study, a rabbit-specific poxvirus, myxoma virus (MYXV), was genetically altered to disrupt multiple members of the poxviral ankyrin-repeat (ANK-R) protein superfamily, M-T5, M148, M149 and M150. A particularly robust activation of the NF-κB pathway was observed in A549 cells following infection with the complete ANK-R knockout (vMyx-ANKsKO). Also, an increased release of IL-6 was only observed upon infection with vMyx-ANKsKO. In virus-infected rabbit studies, vMyx-ANKsKO was the most extensively attenuated and produced the smallest primary lesion of all ANK-R mutant constructs. This study provides the first insights into the shared functions of the poxviral ANK-R protein superfamily *in vitro* and *in vivo*.

Keywords

Myxoma virus; poxvirus; nuclear factor kappa B; interleukin 6; ankyrin-repeat; M-T5; M148; M149; M150; myxomatosis

Introduction

Myxoma virus (MYXV), a rabbit-specific poxvirus, is both an effective vertebrate pest control agent and a promising oncolytic virus candidate (Chan, Rahman, & McFadden, 2013; Kerr, 2012). MYXV, like other poxviruses, has a dsDNA genome flanked with terminal-inverted repeats that is packaged within a large brick-shaped virion. The terminal-inverted repeats and flanking genomic regions contain a large number of immunoregulatory and/or host range genes, which are responsible for determining viral tropism and disease

*Corresponding author: Grant McFadden, Dept of Molecular Genetics and Microbiology, College of Medicine, University of Florida, 1600 SW Archer Road, PO Box 100266, Gainesville, FL 32610, Phone: 352-273-6852, Fax: 352-273-6849.

characteristics (Spiesschaert, McFadden, Hermans, Nauwynck, & Van de Walle, 2011). The functions of numerous MYXV host range genes have been previously reported. In general, the functions of their gene products can be categorized as anti-apoptotic, NF-κB regulators, anti-inflammasome, cytokine inhibitors, signaling modulators, blockers of leukocyte activation or chemotaxis, and serine protease inhibitors (Rahman, Mohamed, Kim, Smallwood, & McFadden, 2009; Spiesschaert et al., 2011). Note that NF-κB signaling can be either induced or inhibited by poxvirus infection, and this signaling can then be either pro-apoptotic or anti-apoptotic depending on the context (Joshi, Francis, Silverman, & Sahni, 2004; Monks, Biswas, & Pardee, 2004; Rahman & McFadden, 2011; Thomas et al., 2002; C. Y. Wang, Mayo, & Baldwin, 1996).

Ankyrin-repeat (ANK-R) motifs are one of the most prevalent protein motifs encoded by eukaryotes. Multiple helix-loop-helix domains within the ANK-R protein unit coalesce and specifically interact with a large variety of target proteins (Li, Mahajan, & Tsai, 2006). Despite the ubiquitous presence of ANK-R proteins in eukaryotes, the ANK-R protein motif is absent in most viruses, except poxviruses (Sonnberg, Fleming, & Mercer, 2011). Phylogenetic analysis has revealed that the poxviral ANK-R protein superfamily members all likely originated from an ancestral ANK-R protein containing both an N-terminal ANK-R domain and a C-terminal Poxvirus Repeat of Ankyrin C-terminus (PRANC) domain (Sonnberg et al., 2011). The unique arrangement of these two domains has only been observed in poxviruses, Rickettsia sp. and parasitoid wasps (Werren et al., 2010). Thus far, multiple poxviruses encode members of this superfamily, such as the orthopoxvirus K1L, CP77, CP006, and G1R gene products, have been identified as inhibitors of the NF-κB pathway (Chang et al., 2009; Mohamed, Rahman, Lanchbury, et al., 2009; Mohamed, Rahman, Rice, et al., 2009; Shisler & Jin, 2004).

The activation of the classical NF-κB pathway is initiated following the detection of certain pro-inflammatory cytokines, damage associated molecular patterns (DAMPs) or pathogen associated molecular patterns (PAMPs) by cellular pattern recognition receptors. The resultant signaling cascade leads to the phosphorylation of a key activator kinase, inhibitor of NF-κB kinase (IKK). The phosphorylation of inhibitor of NF-κB α (IκBα) and p105 by activated IKK leads to their ubiquitination and (complete or partial) degradation. This degradation allows the NF-κB subunits p65 and p50 to dimerize in the cytoplasm, translocate to the nucleus and stimulate the transcription of multiple NF-κB responsive genes. The poxviral ANK-R genes K1L, CP77, CP006 and G1R encode proteins that inhibit the activation of NF-κB by binding to or influencing proteins within this pathway.

MYXV encodes four distinct members of the poxviral ANK-R protein superfamily, called M-T5, M148, M149 and M150. While each of these proteins possess a different number of N-terminal ANK-R domains, they all possess a PRANC C-terminal domain, which binds the cellular adaptor protein Skp1 *in vitro* and *in vivo* (Werden et al., 2009). Skp1 is an important member of the cellular Skp1-cullin-F-box (SCF) complex, which in turn is responsible for ubiquitinating cellular protein targets that regulate key host pathways (such as cell cycle regulation) for proteasome-dependent degradation (Bai et al., 1996). Thus far, at least two functional roles have been uncovered for M-T5. Early studies have reported that M-T5 helps prevent cell cycle arrest and apoptosis during MYXV infection (Johnston et al., 2005;

Mossman, Lee, Barry, Boshkov, & McFadden, 1996). M-T5 appears to modulate the cell cycle by acting as an adaptor between the ubiquitination/proteosomal degradation machinery of the cell and the cell cycle regulator p27/Kip1 (Johnston et al., 2005). vMyx-MT5KO exhibits defective dissemination in rabbits, likely due to an inability of the M-T5-minus virus to suppress apoptosis during T-cell infection (Mossman et al., 1996). More recently, M-T5 has also been found to bind and activate cellular AKT, also known as Protein Kinase B (PKB), by promoting AKT phosphorylation at serine 473 during MYXV infection of cells where this site is underphosphoylated (Werden, Barrett, Wang, Stanford, & McFadden, 2007; Werden et al., 2009). Much less is known about the functions of M148, M149 and M150 during viral infection, although the deletion of individual genes reduces virus virulence in infected rabbits (Blanie, Mortier, Delverdier, Bertagnoli, & Camus-Bouclainville, 2009; Camus-Bouclainville et al., 2004). Some preliminary evidence suggests that M150, also called Myxoma Nuclear Factor (MNF), might be involved in the suppression of NF-κB activation (Camus-Bouclainville et al., 2004).

This study provides the first *in vitro* and *in vivo* comparison between a poxvirus with a complete deletion of the ANK-R protein superfamily, and its wild-type (WT) equivalent. In this study, MYXV constructs lacking all, or a combination of, genes encoding ANK-R proteins were created, purified and characterized. The ANK-R Mutant viruses tested in this study are vMyx-MT5KO (inactivation of both copies of the *M-T5* gene that maps within the TIR region of the vMyx genome), vMyx-148–150KO (deletion of the entire *M148-M149-M150* gene locus near the right TIR), and vMyx-ANKsKO (loss of both copies of *M-T5* plus *M148*, *M149* and *M150*). The initial characterization of these viruses was performed in both a human cell line with a well-characterized and functional NF-κB pathway (A549) and a rabbit T cell line (Liu, Wennier, Zhang, & McFadden, 2011; Mossman et al., 1996; Rahman, Liu, Chan, Rothenburg, & McFadden, 2013). Also, an *in vivo* study in virus-infected rabbits was completed in order to determine the overall impact of the ANK-R protein superfamily on MYXV virulence.

Materials and Methods

Cell lines

Monkey cell line BSC-40 (ATCC# CRL-1658), human cell line A549 (ATCC# CCL-185), and rabbit cell line RK13 (ATCC# CCL-37) were maintained in Dulbecco's Modified Eagle Medium (DMEM; Invitrogen) supplemented with 10% fetal bovine serum (FBS; Gibco), 2 mM L-glutamine, and 100 U/mL of penicillin/streptomycin (pen/strep; Invitrogen). RL-5 cells were cultured in RPMI 1640 medium (Lonza, BioWhittaker) supplemented with 10% FBS, 2 mM L-glutamine, and 100 U/mL of pen/strep. All cultures were maintained in a humidified chamber at 37° C and 5% CO_2. The BSC40 monkey kidney cell line was received as a gift from Richard Condit from the University of Florida. During maintenance, cell cultures were periodically tested to confirm the absence of contaminating mycoplasma species, using a PCR-based assay (Southern Biotech #13100-01)

Viral Preparation

All viruses used in this study were grown and amplified in BSC40 cells. Viruses were purified by centrifugation through a sucrose cushion as described previously (Smallwood, Rahman, Smith, & McFadden, 2010). The viruses in this study were titered in BSC40 cells or in RK13 cells.

Construction of recombinant viruses

The production of vMyx-MT5KO was described previously (Mossman et al., 1996). Two novel ANK-R mutant viruses, vMyx-148–150KO and vMyx-ANKsKO, and three revertant viruses, vMyx-MT5KO Rev, vMyx-148–150KO Rev, and vMyx-ANKsKO Rev, were produced during the course of this study (Table 1). Either recombinant plasmids or recombinant PCR products were constructed to hybridize with specific regions of the MYXV genome. (Figure 1A) To generate vMyx-148–150KO and vMyx-ANKsKO, the construct pDNR222 Δ148–150 DSred2 was created. Overlapping PCR was used to flank a DSred2 expression cassette, driven by a synthetic poxviral early/late promoter, with ~ 1 kb of hybridizing sequence (Chakrabarti, Sisler, & Moss, 1997). These flanking sequences were selected to facilitate the replacement of the M148, M149, and M150 locus of MYXV with a DSred2 expression cassette. The primers used for the amplification of this recombinant PCR product contained flanking attB sequences that enabled the insertion of the PCR product into the Gateway cloning donor vector pDNR222 (Invitrogen) (Table 2) (Figure 1A). vMyx-148–150KO and vMyx-ANKsKO were created by infecting BSC40 cells with either vMyx-WT or vMyx-MT5KO, respectively, followed by transfection with pDNR222 Δ148–150 DSred2 (Figure 1B). Multiple rounds of foci purifications were performed based on DSred2 expression and continued until pure foci were isolated and confirmed by PCR using appropriate primers (Figure 1C and Table 2).

After ANK-R mutant MYXV constructs were purified and confirmed, revertant viruses were made from each knockout virus. The M-T5 sequence in vMyx-MT5KO and vMyx-ANKs-KO was restored by infecting a selectively permissive cell line Caki1, which favors vMyx-WT replication, and subsequently cotransfecting both pBS135-136eGFP (described previously) and a revertant plasmid containing the complete M-T5 sequence with ~ 500 bp flanking genomic sequence (Figure 1A and 1B) (Chakrabarti et al., 1997; Johnston et al., 2003). Multiple rounds of foci purification were performed based on both foci size and eGFP expression.

The 148-149-150 locus was reintroduced into vMyx-148–150KO and the Partial ANKs KO revertant MYXVs through the infection of BSC40 cells followed by transfection with a PCR product containing the ORFs M148–M150 and 1000 bp of flanking genomic sequence (Figure 1A). vMyx-148–150KO revertant viruses were purified in RK13 cells through many rounds of clear plaque selection. The complete vMyx-ANKsKO revertant underwent multiple rounds of foci purification in BSC40s based on eGFP expression in the absence of DSred2 expression. The purity of all newly constructed viruses was confirmed by PCR using appropriate primers (Figure 1A and Table 2).

Single-step growth curves

Cells were seeded into 24-well dishes in semi-confluent monolayers (1.25×10^5 cells) and infected with vMyx-WT or the ANK-R mutant viruses at an MOI of 5 for 1 hour. After 1 hour of incubation, the innoculum was removed, the cell monolayer was washed with PBS and fresh complete media was added to the monolayer. Samples were collected at various times post-infection and stored at −80°C until processed. The samples were freeze-thawed at −80°C and 37°C three times and sonicated for one minute to release virus from infected cells. The virus was titrated on BSC40 cells by serial dilution in triplicate. After 48 hrs of infection, fluorescent foci were counted and the viral titer was calculated.

Immunofluorescence

On rat collagen-coated coverslips, MYXV-permissive human A549 cells (5×10^3) were seeded and either mock infected or infected with vMyx-WT, vMyx-MT5KO, vMyx-148–150KO, or vMyx-ANKsKO for 1 hr at 37°C. After removal of the innoculum, the monolayers were washed with PBS and covered in fresh media. At specified time points post infection, coverslips were washed with PBS and fixed with 4% paraformaldehyde (Sigma) for 15 minutes at 4 degrees Celsius. The fixative was then discarded and excess paraformaldehyde was removed by washing 3X with cold PBS. The coverslip was then blocked with Blocking buffer (5% FBS +PBS +0.3% TritonX-100) for 1 hr at RT. In order to detect the NF-κB p65, the coverslip was incubated with rabbit anti-p65 (sc-372; Santa Cruz) diluted 1:100 in Antibody dilution buffer (1X PBS, 3% BSA/0.3% TritonX 100) overnight at 4 degrees Celsius. Residual primary antibody was removed by three 15 min washes with PBS. A 2 hr RT incubation with Alexafluor 488 (green) goat anti-rabbit antibody diluted 1:1,000 in Antibody dilution buffer was performed next. Another set of PBS washes was executed to remove excess secondary antibody. After p65 labeling, coverslips were mounted on microscope slides with 7.5 μL Vecta-shield hard mounting media with DAPI (4′,6 diamidino-2-phenylindole; Vector Laboratories) for the visualization of nuclei. Cells were viewed using the Leica inverted fluorescent microscope. The localization of p65 was recorded for ~100 cells per sample. Using these data, the percentage of total cells exhibiting a nuclear localization of p65 was calculated.

ELISA

A549 cells (5×10^5) were seeded in 6 well plates. The following day, the cells were mock infected, infected with vMyx-WT, vMyx-MT5KO, vMyx-148–150KO or vMyx-ANKsKO (at MOI of 5), or treated with the TLR agonist Pam2CSK4, which is known to stimulate NF-κB activation in these cells. Supernatants were collected at specified time points post infection. The concentration of IL-6 and IL-8 in the supernatants was determined using Ready-Set-Go! ® ELISA assay kits (eBioscience) following the manufacturer's protocol.

Trypan blue exclusion assays

For trypan blue exclusion assays, A549 cells (5×10^5) were seeded into 6 well plates. The following day, the cells were either mock infected or infected with vMyx-WT, vMyx-MT5KO, vMyx-148–150KO or vMyx-ANKsKO (at MOI of 5). Both detached cells in the supernatant and trypsinized adherent cells were pooled together. After the cells were

pelleted and resuspended in 250 μL of fresh media, the samples were incubated at room temperature for 15 min in a 0.2% solution of trypan blue dye (Sigma). Cytotoxicity was calculated as the percentage of cells permeated with trypan blue divided by the total number of cells.

MTT cell proliferation assays—The relative quantity of viable, proliferating cells after infection was estimated by measuring mitochondrial function using CellTiter 96 Non-Radioactive Cell Proliferation Assay (MTT, Promega). A549 cells (5.0×10^3) were seeded into 96-well dishes and infected with vMyx-WT or the ANK-R mutant viruses (MOI 5) at 24, 48, and 72 hours prior to the execution of the MTT assay. After the first hour of infection, the innoculum was removed, the cell monolayer was washed with PBS and fresh complete media was added. The MTT assay was performed according to the manufacturer's instructions. Each treatment was performed in triplicate and the results provide an indication of the relative quantity of viable/proliferating cells after the different treatments.

TUNEL assay—The proportion of cells undergoing apoptosis during ANK-R mutant virus infection was determined using TUNEL staining to monitor nuclear DNA degradation and flow cytometric analysis. A549 cells (1×10^6) were seeded into 6 well plates. The following day, the cells were either mock infected or infected with vMyx-WT, vMyx-MT5KO, vMyx-148–150KO or vMyx-ANKsKO (MOI of 5). Both detached cells in the supernatant and trypsinized adherent cells were collected and pooled together. Fragmented DNA, a marker for apoptotic cell death, was stained using the In situ Direct DNA Fragmentation (TUNEL) Assay Kit (Abcam, ab66108) according to the manufacturer's protocol. Anti-BrdU APC antibody (eBioscience) was used instead of anti-BrdU Red to allow the simultaneous detection of BrdU and DSred2. The cells were then characterized using a FACScalibur (Becton Dickinson) and analyzed by CELLQuest software. The collected data was analyzed using FCS Express 4 Flow Cytometry software (De Novo Software).

Rabbit experiments

New Zealand White rabbits were purchased from Charles River Laboratories International. This animal study was approved by the Institutional Animal Care and Usage Committee (IACUC) at the University of Florida. This study was performed as described previously (Liu et al., 2011). Briefly, 1000 focus-forming units (FFU) of the tested virus was resuspended in 100 μl of PBS and inoculated intradermally in the left flank of each rabbit. Daily physical examinations were performed to evaluate the condition of the rabbits by monitoring respiration, temperature, heart rate, weight, attitude, lung sound, food and water intake, urine and feces output, hydration status, posture, indications of primary lesion and the appearance of secondary lesions (Table 3). The rabbits receive a daily clinical score (from 0 to 34) that is dependent on observations collected during the daily evaluation. The animals were humanely euthanized when the clinical score reached 26 to 34, had open mouth breathing due to respiratory stress, orthopnea, cyanosis or no food and water intake for 48 hr.

Results

Myxoma virus lacking M-T5 exhibits defective replication in A549 and RL-5 cell lines

Previous studies have indicated that the ability of vMyx-MT5KO to replicate in a variety of test mammalian cell lines is influenced by the basal level of cellular AKT phosphorylation and/or a cellular susceptibility to cell cycle arrest (Johnston et al., 2005; G. Wang et al., 2006). Since the cellular tropism of vMyx-148–150KO and vMyx-ANKsKO has not been investigated, single step growth curves for vMyx-WT, vMyx-MT5KO, vMyx-148–150KO, and vMyx-ANKsKO were performed in a number of cell lines. Both BSC40 (monkey kidney) and RK13 (rabbit kidney) cell lines are known to be highly permissive to MYXV infection. All the viruses tested demonstrated comparable levels of viral replication and production of progeny virus in these cells (Figure 2A and 2C). This confirms that these viruses are capable of optimal replication kinetics under favorable permissive cellular conditions.

The functionality of the NF-κB signaling pathway in the MYXV-permissive human lung cancer cell line A549 makes it an optimal model for the study of potential NF-κB pathway modulators, like the poxviral ANK-R proteins. Single step growth curve analysis within A549 cells revealed a notable defect in the replication of MYXV constructs lacking M-T5 (Figure 2B). The additional deletion of the M148–M150 gene locus did not further alter the ability of the recombinant vMyx-ANKsKO to replicate within A549 cells.

An earlier report by Mossman et. al. reported defective vMyx-MT5KO replication within the rabbit T-cell line, RL5 (Mossman et al., 1996). To determine whether the newly constructed vMyx-148–150KO and vMyx-ANKsKO viruses also exhibited defective replication in RL-5 cells, single-step growth curve analysis was performed in RL-5 cells. In agreement with the published literature, MYXV lacking M-T5 displayed a notable defect in replicative ability within RL-5 cells (Figure 2D). However, the deletion of M148–M150 alone did not appear to affect virus replication in RL-5 cells, nor does it further exacerbate the replication defect observed for the vMyx-MT5KO virus when it is carried within the vMyx-ANKsKO virus.

NF-κB activation is triggered by infection with ANK-R mutant myxoma virus constructs

Although several members of the poxviral ANK-R superfamily have been shown to act as inhibitors of the classical NF-κB pathway, no previous studies have reported NF-κB stimulation during *in vitro* infection with MYXV lacking one or multiple ANK-R proteins (Mohamed, Rahman, Lanchbury, et al., 2009; Mohamed, Rahman, Rice, et al., 2009). Since human A549 cells possess a functional NF-κB pathway and also exhibit a defect in the replication of MYXV lacking M-T5, the ability of vMyx-WT and the ANK-R mutant viruses to stimulate the NF-κB pathway in A549 cells was tested. The translocation of the endogenous NF-κB subunit p65 from the cytoplasm to the nucleus of a cell is indicative of the activation of the classical NF-κB pathway. The nuclear accumulation of p65 in A549 cells after infection with the various ANK-R mutant viruses was assessed via immunofluorescence. Overall, vMyx-ANKsKO infection of A549 cells triggered the nuclear accumulation of p65 in a higher percentage of cells than vMyx-WT, vMyx-MT5KO or

vMyx-148–150KO infections (Figure 3A). The disparity between the ability of vMyx-WT and the ANK-R Mutant infections to stimulate NF-κB activation was observed as early as 2 hrs after infection and was most dramatic at 12 hours post infection. Relative to vMyx-WT infection, the percentage of A549 cells with nuclear accumulation of p65 after 12 hours of vMyx-MT5KO, vMyx-148–150KO, and vMyx-ANKsKO virus infection (MOI 5) increased approximately 40, 20, and 120 fold, respectively. A representative image produced after immunofluorescence for p65 in A549 cells following 12 hours of mock, vMyx-WT or vMyx-ANKsKO infection is shown (Figure 3B). A majority of cells within the monolayer after mock or vMyx-WT infection exhibit segregation between p65 (green anti-p65 immunoflourescence) and nuclei (blue DAPI.) In contrast, most cells within a monolayer infected with vMyx-ANKsKO demonstrate extensive co-localization between p65 and the nucleus.

Infection with ANKs knockout myxoma virus triggers an increase in both IL-6 and IL-8 release

Previous studies have reported that the activation of the NF-κB pathway within A549 cells by various ssRNA viruses leads to the secretion of IL-8 and/or IL-6 (Arnold, Humbert, Werchau, Gallati, & Konig, 1994; Bao et al., 2007; Chun et al., 2013; Devhare, Chatterjee, Arankalle, & Lole, 2013; Julkunen et al., 2000; Kanzawa et al., 2006). Interestingly, all the ANK-R mutant MYXV constructs also stimulate NF-κB activation in A549 cells, but to varying degrees. Further experiments with ANK-R mutant MYXV constructs were performed to determine if, as in the case of ssRNA virus infections, an increased release of IL-8 and/or IL-6 accompanies the virus-induced NF-κB stimulation. Following vMyx-ANKsKO infection, a slight delay in IL-8 and IL-6 protein secretion occurred relative to the kinetics of NF-κB stimulation. Specifically, vMyx-ANKsKO infection led to an increased release of IL-8 at 48, 72 and 96 HPI compared to vMyx-WT infection (Figure 4A). vMyx-ANKsKO infection also stimulated an increased secretion of IL-6 at 72 and 96 HPI (Figure 4B). In contrast, vMyx-148–150KO infection did not stimulate the release of IL-6. However, vMyx-148–150KO infection did increase the release of IL-8 at 72 and 96 HPI. Unexpectedly, vMyx-MT5KO infection did not promote the secretion of either IL-8 or IL-6 (Figure 4A and 4B). If anything, the secretion of IL-8 and IL-6 appears to be reduced in vMyx-MT5KO infected cells relative to vMyx-WT infected cells.

Infection of A549 cells with myxoma virus lacking M-T5 results in excessive cytotoxicity and apoptosis

Early studies of M-T5 have described the anti-apoptotic function of M-T5 *in vitro* (Johnston et al., 2005). In order to determine the effect of ANK-R mutant MYXV infections on cell viability, trypan blue exclusion assays, MTT assays and TUNEL assays were performed at various time points post infection. At both 24 and 48 HPI, vMyx-MT5KO and vMyx-ANKsKO infection caused a ~5 fold increase in cytotoxicity relative to vMyx-148–150KO or vMyx-WT infection, as measured by the exclusion of trypan blue (Figure 5A). Curiously, during infection with all tested myxoma viruses, the MTT assay detected a similar decrease in the quantity of active mitochondrial metabolism in A549 cells at 24 and 48 HPI (Figure 5B). This could indicate that viable cells infected with vMyx-WT or vMyx-148–150KO exhibit retarded proliferation. By 72 HPI, the number of cells with actively metabolic

mitochondria does begin to decrease during infection with vMyx-MT5KO and vMyx-ANKsKO, relative to vMyx-148–150KO or vMyx-WT infection. While the trypan blue exclusion assay gives a rough estimate of cell viability as assessed by cell membrane permeability, it does not specify the mechanism of cell death and often overestimates cytotoxicity. TUNEL assays were performed to determine if virus-induced apoptosis contributes to the number of dead cells observed during vMyx-MT5KO and vMyx-ANKsKO infection (Figure 6A and 6B). As expected, A549 cells infected with vMyx-MT5KO or vMyx-ANKsKO underwent more apoptosis than cells infected with vMyx-WT or vMyx-148–150KO (Figure 6B). Interestingly, the proportion of cells undergoing apoptosis is 2-fold higher during infection with vMyx-MT5KO relative to vMyx-ANKsKO. This suggests that, while M-T5 reduces the level of apoptosis in infected cells, one or more members of the M148–M150 family might in fact contribute to the virus-mediated induction of apoptosis.

ANK-R knockout myxoma virus infection of NZW rabbits is severely attenuated

In vivo infection studies in NZW rabbits were previously reported for vMyx-MT5KO, vMyx-148KO, vMyx-149KO, vMyx-150KO, and vMyx148–149KO MYXV constructs (Blanie et al., 2009; Camus-Bouclainville et al., 2004; Mossman et al., 1996). Each of these viruses were attenuated, in varying degrees, relative to vMyx-WT infection. At the time of writing, no previous reports have examined the impact of selectively deleting the entire ANK-R protein superfamily on poxviral virulence. In this study, vMyx-148–150KO (lacking the three unique single copy ANK-R genes) and vMyx-ANKsKO (mutant for all 5 ANK-R genes) were tested for virulence in NZW rabbits. vMyx-WT, vMyx-MT5KO, vMyx-MT5KO Rev, vMyx-148–150KO Rev and vMyx-ANKsKO Rev infections were also performed in parallel. In congruence with previous findings, vMyx-WT and all the revertant MYXV inoculations of NZW rabbits resulted in a rapid, wide-spread and fatal infection. Within four days of inoculation of vMyx-WT and the revertant MYXVs, a sizable primary lesion and minute secondary lesions (5/8 rabbits) were apparent (Table 4). By the seventh day of infection, the lesions became more severe and numerous. Also, the majority of these infected rabbits developed a mucosal bacterial infection (7/8). Ultimately, at 9–10 days post inoculation, the animals had to be euthanized due to the increasing severity of clinical symptoms, according to IACUC regulations (Table 3). Comparatively, vMyx-148–150KO infection was much less severe than vMyx-WT or revertant infections (Figure 7B). More specifically, the size/number of lesions and the severity of the mucosal bacterial infections were diminished during vMyx-148–150KO infection. Despite this attenuation, vMyx-148–150KO infection displayed a similar progression of symptoms within the first 7 DPI as WT or revertant infections. However, while vMyx-WT infection symptoms rapidly intensified after 7 days, vMyx-148–150KO infection began showing signs of healing after 7 DPI and all rabbits recovered fully within 17 DPI.

Mossman et. al. previously determined that vMyx-MT5KO infection in NZW rabbits exhibited both reduced lesion size and an almost complete absence of viral dissemination to secondary sites (Mossman et al., 1996). In this study, our observations during vMyx-MT5KO infection were consistent with this previous report (Table 4, Figure 7A). Overall, these *in vivo* observations demonstrate that knocking out M-T5 alone produced a more

severe viral attenuation than knocking out M148, M149 and M150 individually or together (Blanie et al., 2009; Camus-Bouclainville et al., 2004; Mossman et al., 1996). Since M148 KO, M149 KO, M150 KO and MT5KO MYXV constructs were all attenuated in rabbits, vMyx-ANKsKO was predicted to also be attenuated. Indeed, *in vivo* ANKs KO infection produced smaller primary lesions than either vMyx-148–150KO or vMyx-MT5KO infection (Figure 7A). Also, vMyx-ANKsKO, like vMyx-MT5KO, was defective in systemic viral dissemination (Table 4).

Discussion and Conclusions

This study reports that the MYXV gene M-T5 is required for the optimal replication of the virus in both human A549 and in rabbit RL-5 cells (Figure 2). This defective replication was associated with excessive cytotoxicity and apoptosis in A549 cells during infection with MYXV lacking M-T5 (Figure 5A, Figure 6B). These findings are consistent with an earlier study that demonstrated defective MYXV replication and apoptosis in rabbit RL-5 cells infected with vMyx-MT5KO (Mossman et al., 1996). In contrast, the triple deletion of M148-M149-M150 from MYXV had no effect on viral replication or cell viability in either of these cell lines. Thus, the ability of M-T5 to prevent apoptosis, as measured by the TUNEL assay, appears to be unique among the poxviral ANK-R proteins encoded by MYXV. Interestingly, the vMyx-ANKsKO virus induces less apoptosis than the vMyx-MT5KO (Figure 6B), suggesting that, while M-T5 inhibits the induction of apoptosis, one or members of the M148–M150 family might in fact be virus-encoded stimulators of apoptosis.

Prior to this study, a number of poxviral ANK-R proteins and cellular ANK-R proteins have been shown to prevent the activation of NF-κB signaling (Basith, Manavalan, Gosu, & Choi, 2013; Mohamed, Rahman, Lanchbury, et al., 2009; Mohamed, Rahman, Rice, et al., 2009; Rahman & McFadden, 2011). This study provides the first evidence that MYXV ANK-R proteins block NF-κB activation during late stages of infection. Relative to vMyx-WT infection, vMyx-MT5KO, vMyx-148–150KO and vMyx-ANKsKO infection, at 12 HPI, increased the percentage of A549 cells that exhibit nuclear accumulation of the NF-κB p65 subunit by 40, 20 and 120 fold, respectively (Figure 3A). Since p65 migration from the cytoplasm to the nucleus is a classical indicator for the activation of the NF-κB signaling cascade, these data indicate that the collective function of the MYXV ANK-R proteins is to block or reduce NF-κB activation in infected cells. The dramatic increase in the number of NF-κB-stimulated cells after vMyx-ANKsKO infection, relative to both vMyx-MT5KO and vMyx-148–150KO, indicates that there is some redundancy in the ability of MYXV ANK-R proteins to prevent NF-κB activation during virus infection. Thus, the deletion of the entire ANK-R superfamily is necessary to investigate the cumulative impact of these viral proteins on NF-κB repression.

Thus far, we have shown that ANK-R mutant MYXV infection can both activate NF-κB and engender virus-induced apoptosis. This joint activation of NF-κB and increased cell death upon viral infection has also been observed after infection of A549 cells with ssRNA viruses, such as Respiratory Syncytial Virus and Influenza A virus (Thomas et al., 2002; Tripathi et al., 2013) These previous studies have also observed an increased secretion of IL-8 and IL-6 after viral infection. In this study, vMyx-ANKsKO infection, but not vMyx-

MT5KO infection, was found to stimulate the release of both IL-8 and IL-6 in A549 cells (Figure 4A and 4B). Preliminary evidence suggests that both vMyx-MT5KO and vMyx-ANKsKO infection also increases IL-6 and IL-8 gene expression in the rabbit T-cell line RL-5 (data not shown).

Given the ability of ANK-R mutant MYXV constructs to trigger defined anti-viral pathways like the classical NF-κB pathway and the apoptotic pathway *in vitro*, it is reasonable to hypothesize that these viruses will also be more susceptible to overall anti-viral responses in infected rabbits *in vivo*. Previously, the reduced secondary spread of vMyx-MT5KO *in vivo* was shown to be reflected by the induction of apoptosis in rabbit T-cells upon infection with vMyx-MT5KO (Mossman et al., 1996). Similarly, vMyx-ANKsKO infection does not spread beyond the primary lesion (Table 4). Although both vMyx-MT5KO and vMyx-ANKsKO are restricted to the primary site of infection, the primary lesion produced during vMyx-ANKsKO infection was notably smaller than the lesion produced by vMyx-MT5KO infection (Figure 7A). Thus, vMyx-ANKsKO could be even further limited by additional anti-viral responses within the primary lesion.

This study provides the first evidence that NF-κB activation can be simultaneously suppressed by multiple poxviral ANK-R proteins. A variety of *in vivo* studies have demonstrated that poxviruses unable to properly suppress NF-κB activity are often attenuated in the infected host (Harte et al., 2003; Mohamed, Rahman, Rice, et al., 2009; Rahman et al., 2009; Stack et al., 2005). Further *in vitro* infection studies in primary rabbit cells and histological studies in NZW rabbits will be required to confirm that the increased activation of the NF-κB pathway is a key *in situ* target that contributes to vMyx-ANKsKO attenuation *in vivo*.

This study demonstrates that vMyx-ANKsKO induces a greater innate immune response *in vitro* than vMyx-WT or the other tested ANK-R mutant constructs. Given the close link between innate immune stimulation and the acquisition of long-term acquired immunity, we propose that the vMyx-ANKsKO virus will also induce higher levels of cellular and/or humoral immune responses. In the field of oncolytic virotherapy, a concerted effort has been undertaken to generate safe oncolytic viruses that trigger an enhanced immune response to tumoral antigens that become revealed by virtue of virus replication within tumor beds (Russell, Peng, & Bell, 2012). These newer-generation viruses, through selective infection and replication within tumors, must also counteract the immunosuppressive microenvironment frequently found within most tumors. Previous clinical trials have shown that some oncolytic viruses capable of eliciting anti-tumoral immune responses also increase serum levels of multiple pro-inflammatory cytokines, including IL-6 (Kirn, 2001; Prestwich et al., 2008; Zeh & Bartlett, 2002). Additional studies will be required to determine if the apparently pro-immunogenic vMyx-ANKsKO virus is also an effective oncolytic virus that also favors increased immune responses to tumor antigens.

Acknowledgments

Funding for this study was provided by a NIAID R01 grant AI080607 on MYXV host range genes. We would like to thank Dorothy Smith for help with the animal studies, and Sherin Smallwood for assisting in the IACUC approval process.

References

Arnold R, Humbert B, Werchau H, Gallati H, Konig W. Interleukin-8, interleukin-6, and soluble tumour necrosis factor receptor type I release from a human pulmonary epithelial cell line (A549) exposed to respiratory syncytial virus. Immunology. 1994; 82(1):126–133. [PubMed: 7519169]

Bai C, Sen P, Hofmann K, Ma L, Goebl M, Harper JW, Elledge SJ. SKP1 connects cell cycle regulators to the ubiquitin proteolysis machinery through a novel motif, the F-box. Cell. 1996; 86(2):263–274. [PubMed: 8706131]

Bao X, Liu T, Spetch L, Kolli D, Garofalo RP, Casola A. Airway epithelial cell response to human metapneumovirus infection. Virology. 2007; 368(1):91–101.10.1016/j.virol.2007.06.023 [PubMed: 17655903]

Basith S, Manavalan B, Gosu V, Choi S. Evolutionary, structural and functional interplay of the IkappaB family members. PLoS One. 2013; 8(1):e54178.10.1371/journal.pone.0054178 [PubMed: 23372681]

Blanie S, Mortier J, Delverdier M, Bertagnoli S, Camus-Bouclainville C. M148R and M149R are two virulence factors for myxoma virus pathogenesis in the European rabbit. Vet Res. 2009; 40(1): 11.10.1051/vetres:2008049 [PubMed: 19019281]

Camus-Bouclainville C, Fiette L, Bouchiha S, Pignolet B, Counor D, Filipe C, Messud-Petit F. A virulence factor of myxoma virus colocalizes with NF-kappaB in the nucleus and interferes with inflammation. J Virol. 2004; 78(5):2510–2516. [PubMed: 14963153]

Chakrabarti S, Sisler JR, Moss B. Compact, synthetic, vaccinia virus early/late promoter for protein expression. Biotechniques. 1997; 23(6):1094–1097. [PubMed: 9421642]

Chan WM, Rahman MM, McFadden G. Oncolytic myxoma virus: the path to clinic. Vaccine. 2013; 31(39):4252–4258.10.1016/j.vaccine.2013.05.056 [PubMed: 23726825]

Chang SJ, Hsiao JC, Sonnberg S, Chiang CT, Yang MH, Tzou DL, Chang W. Poxvirus host range protein CP77 contains an F-box-like domain that is necessary to suppress NF-kappaB activation by tumor necrosis factor alpha but is independent of its host range function. J Virol. 2009; 83(9):4140–4152.10.1128/JVI.01835-08 [PubMed: 19211746]

Chun YH, Park JY, Lee H, Kim HS, Won S, Joe HJ, Lee JS. Rhinovirus-Infected Epithelial Cells Produce More IL-8 and RANTES Compared With Other Respiratory Viruses. Allergy Asthma Immunol Res. 2013; 5(4):216–223.10.4168/aair.2013.5.4.216 [PubMed: 23814675]

Devhare PB, Chatterjee SN, Arankalle VA, Lole KS. Analysis of antiviral response in human epithelial cells infected with hepatitis E virus. PLoS One. 2013; 8(5):e63793.10.1371/journal.pone.0063793 [PubMed: 23671700]

Harte MT, Haga IR, Maloney G, Gray P, Reading PC, Bartlett NW, O'Neill LA. The poxvirus protein A52R targets Toll-like receptor signaling complexes to suppress host defense. J Exp Med. 2003; 197(3):343–351. [PubMed: 12566418]

Johnston JB, Barrett JW, Chang W, Chung CS, Zeng W, Masters J, McFadden G. Role of the serine-threonine kinase PAK-1 in myxoma virus replication. J Virol. 2003; 77(10):5877–5888. [PubMed: 12719581]

Johnston JB, Wang G, Barrett JW, Nazarian SH, Colwill K, Moran M, McFadden G. Myxoma virus M-T5 protects infected cells from the stress of cell cycle arrest through its interaction with host cell cullin-1. J Virol. 2005; 79(16):10750–10763.10.1128/JVI.79.16.10750-10763.2005 [PubMed: 16051867]

Joshi SG, Francis CW, Silverman DJ, Sahni SK. NF-kappaB activation suppresses host cell apoptosis during Rickettsia rickettsii infection via regulatory effects on intracellular localization or levels of apoptogenic and anti-apoptotic proteins. FEMS Microbiol Lett. 2004; 234(2):333–341.10.1016/j.femsle.2004.03.046 [PubMed: 15135541]

Julkunen I, Melen K, Nyqvist M, Pirhonen J, Sareneva T, Matikainen S. Inflammatory responses in influenza A virus infection. Vaccine. 2000; 19(Suppl 1):S32–37. [PubMed: 11163460]

Kanzawa N, Nishigaki K, Hayashi T, Ishii Y, Furukawa S, Niiro A, Kannagi M. Augmentation of chemokine production by severe acute respiratory syndrome coronavirus 3a/X1 and 7a/X4 proteins through NF-kappaB activation. FEBS Lett. 2006; 580(30):6807–6812.10.1016/j.febslet.2006.11.046 [PubMed: 17141229]

Kerr PJ. Myxomatosis in Australia and Europe: a model for emerging infectious diseases. Antiviral Res. 2012; 93(3):387–415.10.1016/j.antiviral.2012.01.009 [PubMed: 22333483]

Kirn D. Oncolytic virotherapy for cancer with the adenovirus dl1520 (Onyx-015): results of phase I and II trials. Expert Opin Biol Ther. 2001; 1(3):525–538.10.1517/14712598.1.3.525 [PubMed: 11727523]

Li J, Mahajan A, Tsai MD. Ankyrin repeat: a unique motif mediating protein-protein interactions. Biochemistry. 2006; 45(51):15168–15178.10.1021/bi062188q [PubMed: 17176038]

Liu J, Wennier S, Zhang L, McFadden G. M062 is a host range factor essential for myxoma virus pathogenesis and functions as an antagonist of host SAMD9 in human cells. J Virol. 2011; 85(7): 3270–3282.10.1128/JVI.02243-10 [PubMed: 21248034]

Mohamed MR, Rahman MM, Lanchbury JS, Shattuck D, Neff C, Dufford M, McFadden G. Proteomic screening of variola virus reveals a unique NF-kappaB inhibitor that is highly conserved among pathogenic orthopoxviruses. Proc Natl Acad Sci U S A. 2009; 106(22):9045–9050.10.1073/pnas.0900452106 [PubMed: 19451633]

Mohamed MR, Rahman MM, Rice A, Moyer RW, Werden SJ, McFadden G. Cowpox virus expresses a novel ankyrin repeat NF-kappaB inhibitor that controls inflammatory cell influx into virus-infected tissues and is critical for virus pathogenesis. J Virol. 2009; 83(18):9223–9236.10.1128/JVI.00861-09 [PubMed: 19570875]

Monks NR, Biswas DK, Pardee AB. Blocking anti-apoptosis as a strategy for cancer chemotherapy: NF-kappaB as a target. J Cell Biochem. 2004; 92(4):646–650.10.1002/jcb.20080 [PubMed: 15211562]

Mossman K, Lee SF, Barry M, Boshkov L, McFadden G. Disruption of M-T5, a novel myxoma virus gene member of poxvirus host range superfamily, results in dramatic attenuation of myxomatosis in infected European rabbits. J Virol. 1996; 70(7):4394–4410. [PubMed: 8676463]

Prestwich RJ, Harrington KJ, Pandha HS, Vile RG, Melcher AA, Errington F. Oncolytic viruses: a novel form of immunotherapy. Expert Rev Anticancer Ther. 2008; 8(10):1581–1588.10.1586/14737140.8.10.1581 [PubMed: 18925850]

Rahman MM, Liu J, Chan WM, Rothenburg S, McFadden G. Myxoma virus protein M029 is a dual function immunomodulator that inhibits PKR and also conscripts RHA/DHX9 to promote expanded host tropism and viral replication. PLoS Pathog. 2013; 9(7):e1003465.10.1371/journal.ppat.1003465 [PubMed: 23853588]

Rahman MM, McFadden G. Modulation of NF-kappaB signalling by microbial pathogens. Nat Rev Microbiol. 2011; 9(4):291–306.10.1038/nrmicro2539 [PubMed: 21383764]

Rahman MM, Mohamed MR, Kim M, Smallwood S, McFadden G. Co-regulation of NF-kappaB and inflammasome-mediated inflammatory responses by myxoma virus pyrin domain-containing protein M013. PLoS Pathog. 2009; 5(10):e1000635.10.1371/journal.ppat.1000635 [PubMed: 19851467]

Russell SJ, Peng KW, Bell JC. Oncolytic virotherapy. Nat Biotechnol. 2012; 30(7):658–670.10.1038/nbt.2287 [PubMed: 22781695]

Shisler JL, Jin XL. The vaccinia virus K1L gene product inhibits host NF-kappaB activation by preventing IkappaBalpha degradation. J Virol. 2004; 78(7):3553–3560. [PubMed: 15016878]

Smallwood SE, Rahman MM, Smith DW, McFadden G. Myxoma virus: propagation, purification, quantification, and storage. Curr Protoc Microbiol. 2010; Chapter 14(Unit 14A): 11.10.1002/9780471729259.mc14a01s17

Sonnberg S, Fleming SB, Mercer AA. Phylogenetic analysis of the large family of poxvirus ankyrin-repeat proteins reveals orthologue groups within and across chordopoxvirus genera. J Gen Virol. 2011; 92(Pt 11):2596–2607.10.1099/vir.0.033654-0 [PubMed: 21752962]

Spiesschaert B, McFadden G, Hermans K, Nauwynck H, Van de Walle GR. The current status and future directions of myxoma virus, a master in immune evasion. Vet Res. 2011; 42:76.10.1186/1297-9716-42-76 [PubMed: 21658227]

Stack J, Haga IR, Schroder M, Bartlett NW, Maloney G, Reading PC, Bowie AG. Vaccinia virus protein A46R targets multiple Toll-like-interleukin-1 receptor adaptors and contributes to virulence. J Exp Med. 2005; 201(6):1007–1018.10.1084/jem.20041442 [PubMed: 15767367]

Thomas KW, Monick MM, Staber JM, Yarovinsky T, Carter AB, Hunninghake GW. Respiratory syncytial virus inhibits apoptosis and induces NF-kappa B activity through a phosphatidylinositol 3-kinase-dependent pathway. J Biol Chem. 2002; 277(1):492–501.10.1074/jbc.M108107200 [PubMed: 11687577]

Tripathi S, Batra J, Cao W, Sharma K, Patel JR, Ranjan P, Lal SK. Influenza A virus nucleoprotein induces apoptosis in human airway epithelial cells: implications of a novel interaction between nucleoprotein and host protein Clusterin. Cell Death Dis. 2013; 4:e562.10.1038/cddis.2013.89 [PubMed: 23538443]

Wang CY, Mayo MW, Baldwin AS Jr. TNF- and cancer therapy-induced apoptosis: potentiation by inhibition of NF-kappaB. Science. 1996; 274(5288):784–787. [PubMed: 8864119]

Wang G, Barrett JW, Stanford M, Werden SJ, Johnston JB, Gao X, McFadden G. Infection of human cancer cells with myxoma virus requires Akt activation via interaction with a viral ankyrin-repeat host range factor. Proc Natl Acad Sci U S A. 2006; 103(12):4640–4645.10.1073/pnas.0509341103 [PubMed: 16537421]

Werden SJ, Barrett JW, Wang G, Stanford MM, McFadden G. M-T5, the ankyrin repeat, host range protein of myxoma virus, activates Akt and can be functionally replaced by cellular PIKE-A. J Virol. 2007; 81(5):2340–2348.10.1128/JVI.01310-06 [PubMed: 17151107]

Werden SJ, Lanchbury J, Shattuck D, Neff C, Dufford M, McFadden G. The myxoma virus m-t5 ankyrin repeat host range protein is a novel adaptor that coordinately links the cellular signaling pathways mediated by Akt and Skp1 in virus-infected cells. J Virol. 2009; 83(23):12068–12083.10.1128/JVI.00963-09 [PubMed: 19776120]

Werren JH, Richards S, Desjardins CA, Niehuis O, Gadau J, Colbourne JK, Gibbs RA. Functional and evolutionary insights from the genomes of three parasitoid Nasonia species. Science. 2010; 327(5963):343–348.10.1126/science.1178028 [PubMed: 20075255]

Zeh HJ, Bartlett DL. Development of a replication-selective, oncolytic poxvirus for the treatment of human cancers. Cancer Gene Ther. 2002; 9(12):1001–1012.10.1038/sj.cgt.7700549 [PubMed: 12522439]

Highlights

- Deletion of all ANK-R genes from MYXV caused robust activation of the NF-κB pathway.
- Increased release of IL-6 was only observed upon infection with vMyx-ANKsKO.
- Deletion of all ANK-R genes caused extensive attenuation of MYXV in rabbits.
- First report on shared functions of the poxviral ANK-R protein superfamily.

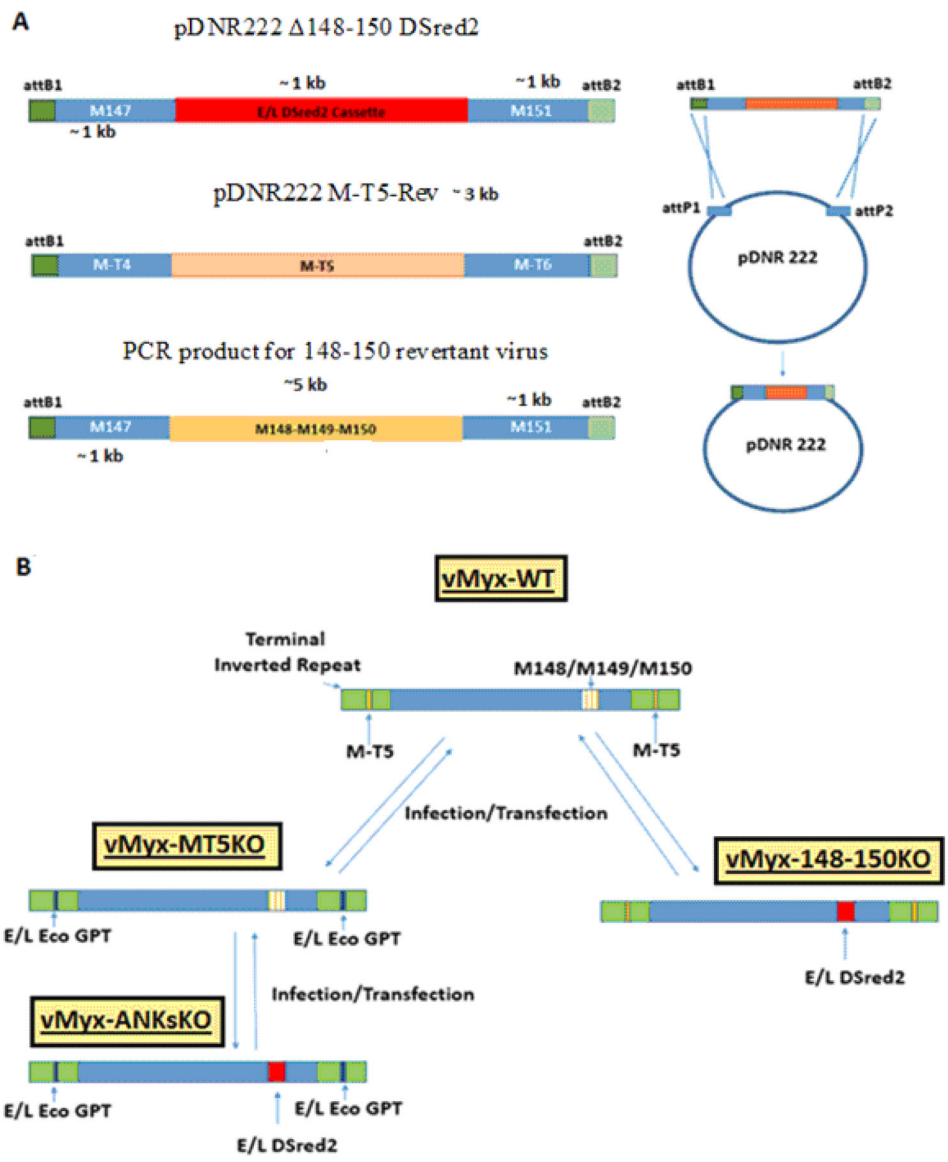

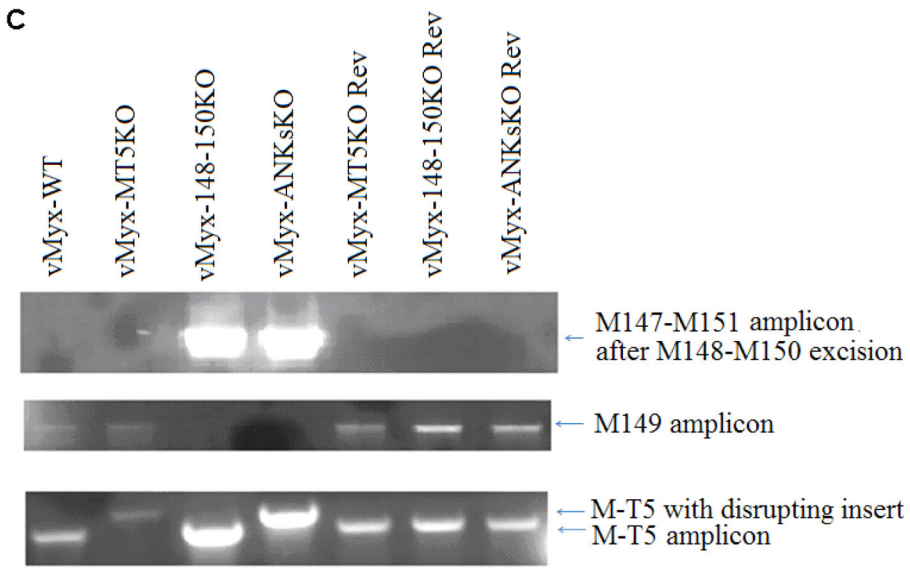

Figure 1. Construction of ANK-R mutant and revertant myxoma viruses

A) Using overlapping PCR and Gateway cloning technology, recombinant plasmids were synthesized to produce ANK-R mutant and revertant viruses. pDNR222 Δ148–150 DSred2 was designed to replace the MYXV 148–150 locus, excluding 150 bp of the flanking sequence, with a dsRed2 expression cassette driven by a poxviral early-late promoter p7.5. pDNR222 M-T5-Rev, containing M-T5 and 500 bp of flanking genomic MYXV sequence, was used to generate the vMyx-MT5KO revertant virus and a partial vMyx-ANKsKO revertant virus. To create these plasmids, PCR products were cloned into pDNR222 using the Gateway Cloning System. To produce the vMyx-148–150KO revertant and the vMyx-ANKsKO revertant, a ~7 kb amplicon was generated. This PCR product was used directly during infection/transfection to generate revertant virus. B) The production of vMyx-MT5KO was previously described by Mossman et. al (Mossman et al., 1996). vMyx-148–150KO and vMyx-ANKsKO were synthesized by infecting BSC40 cells with either vMyx-WT or vMyx-MT5KO, respectively, followed by transfection with pDNR222 Δ148–150 DSred2. C) PCR was performed to confirm the genotypes of the newly synthesized ANK-R mutant myxoma viruses and revertant viruses. Genotyping primer sequences are reported in Table 2.

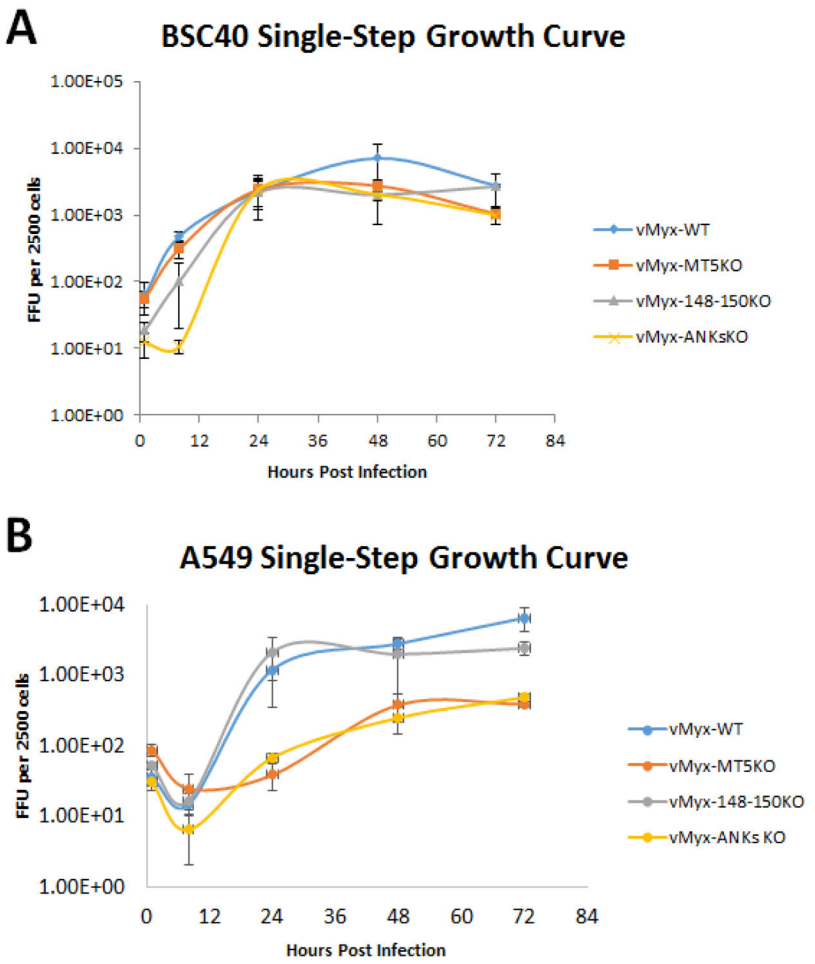

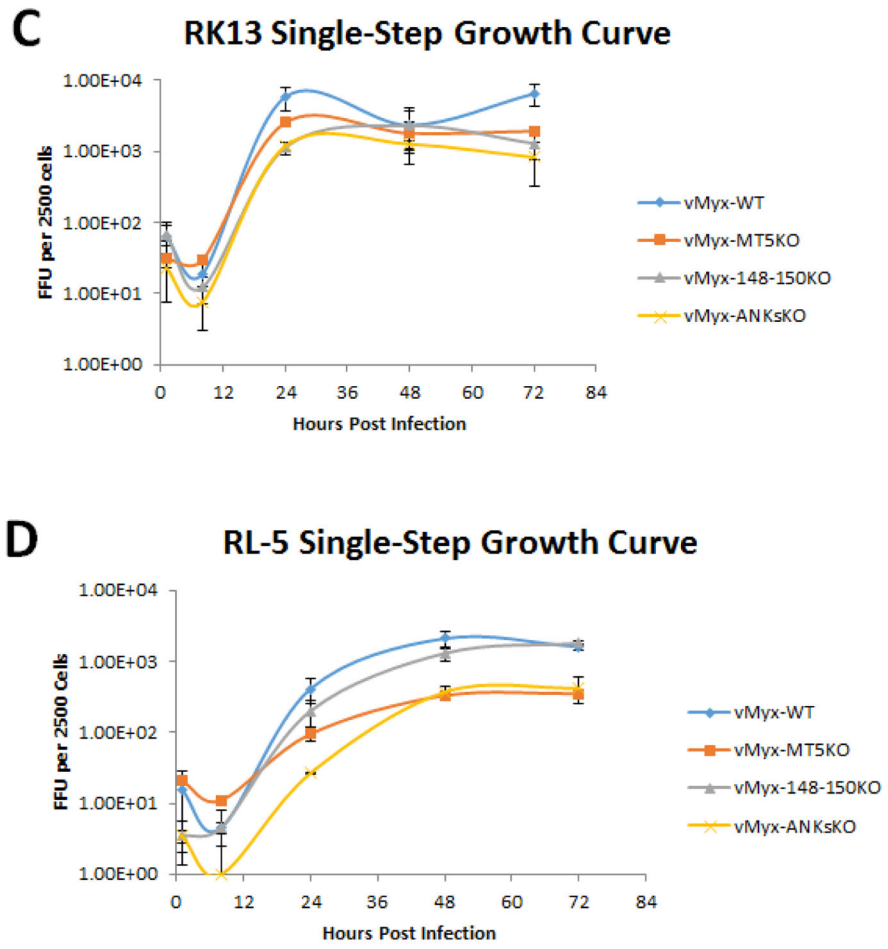

Figure 2. Myxoma virus lacking M-T5 exhibits defective replication in A549 (human lung carcinoma cell line) and RL-5 (rabbit T-cell line)

The ability of vMyx-WT, vMyx-MT5KO, vMyx-148–150KO, and vMyx-ANKsKO to replicate in various cell lines was determined by single-step growth analyses (MOI 5). Two MYXV-permissive cell lines, BSC40 (Monkey kidney) and RK13 (Rabbit kidney) (A and C) and two test cell lines, human A549 and rabbit RL-5 (B and D) were tested. Viral titers were assessed by focus formation assay. Values are expressed as the mean FFU per 2500 cells (± standard deviation [SD]) from triplicate experiments.

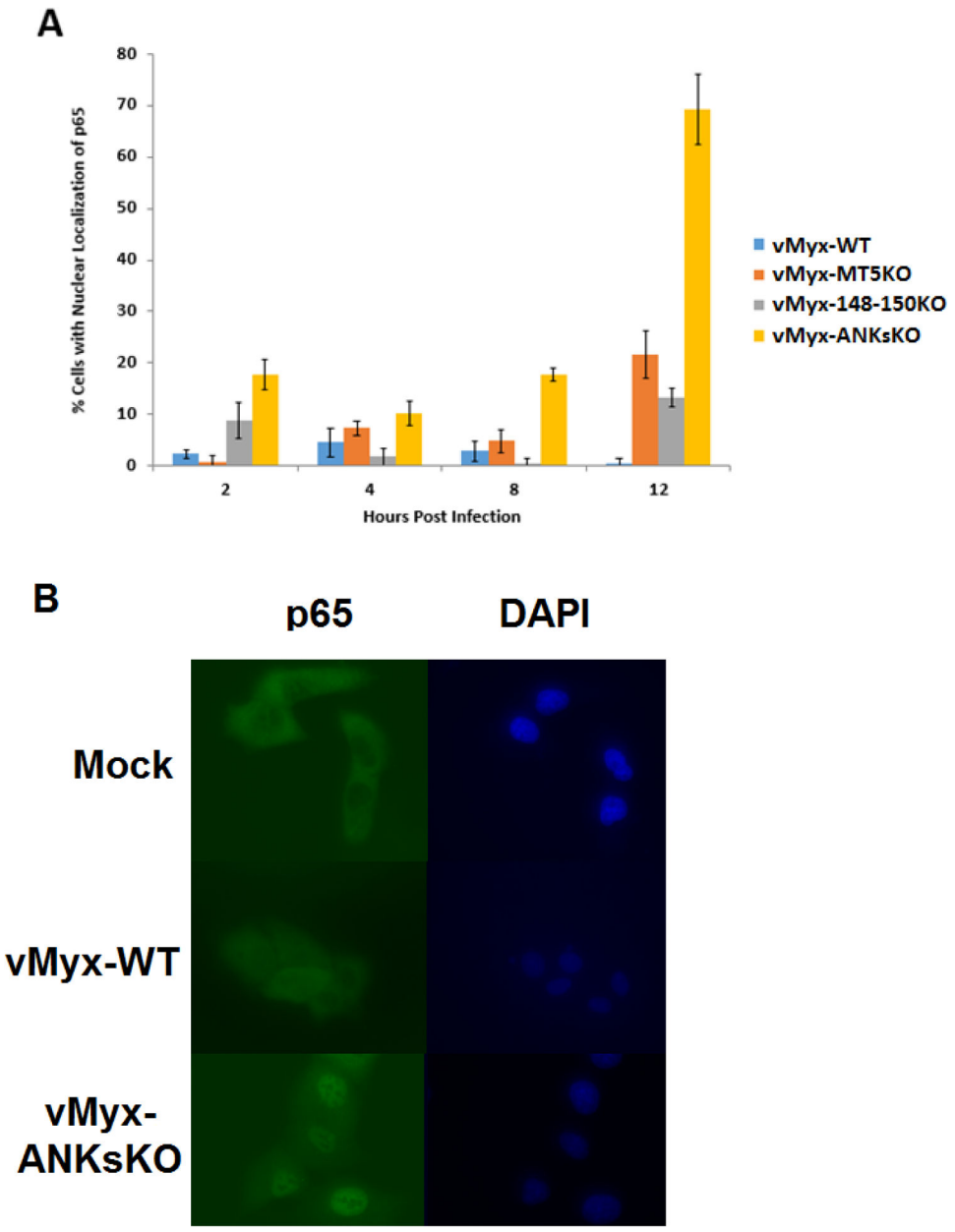

Figure 3. Absence of all the ANK-Rs from MYXV stimulates excessive nuclear accumulation of p65 in A549 cells

The cellular localization of the NF-κB subunit p65 was assayed in A549 cells infected with vMyx-WT, vMyx-MT5KO, vMyx-148–150KO, or vMyx-ANKsKO viruses (MOI 5) at 2, 4, 8, and 12 hours post infection. Nuclei (blue) were detected using DAPI staining. Endogenous p65 (green) was detected through indirect immunofluorescence and fluorescent microscopy analysis. A) The percentage of total cells with a nuclear localization of p65 throughout virus infection, out of ~100 observed cells, is displayed above. Values are expressed as the mean percentage of cells with a nuclear localization of p65 (± standard deviation [SD]) from triplicate experiments. B) Representative images of A549 cell monolayers at 12 hours post mock, vMyx-WT, or vMyx-ANKsKO infection.

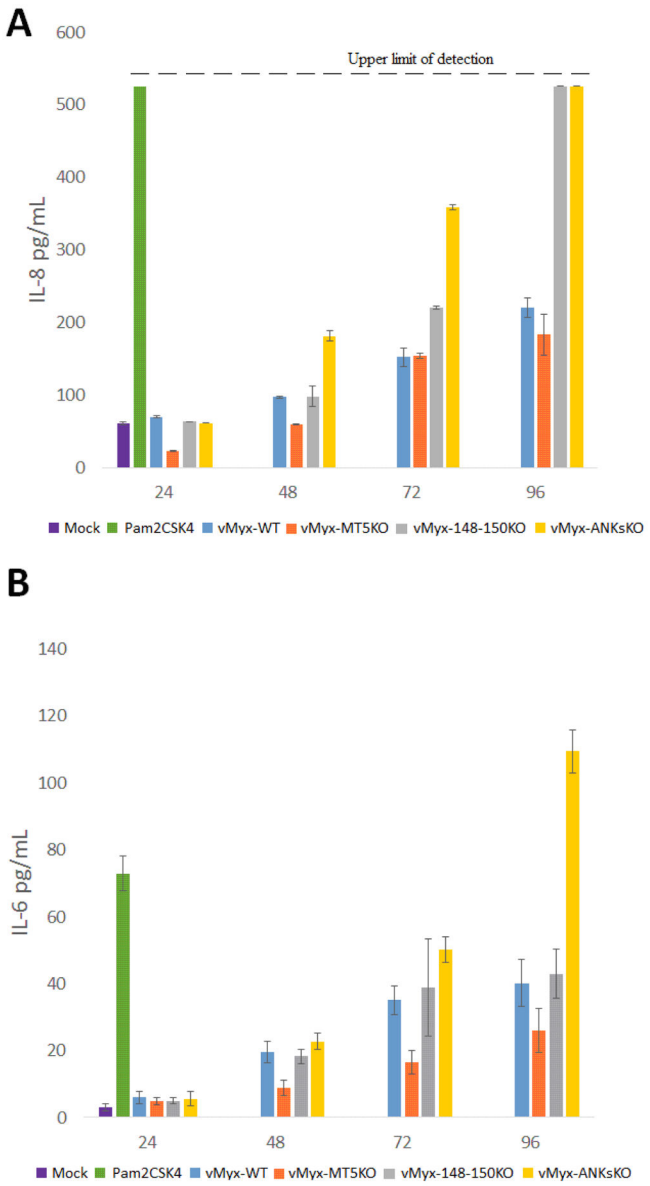

Figure 4. Kinetics of cytokine secretion in myxoma virus infected A549 cells *in vitro*

A549 cells were mock infected, treated with Pam2CSK4 (a TLR4 agonist active for A549 cells) or infected with vMyx-WT, vMyx-MT5KO, vMyx-148–150KO, or vMyx-ANKsKO viruses. Cell supernatants were collected at indicated time points to measure secretion of A) IL-8 and B) IL-6 by ELISA. Values are expressed as mean cytokine concentration (± standard deviation [SD]) from triplicate experiments.

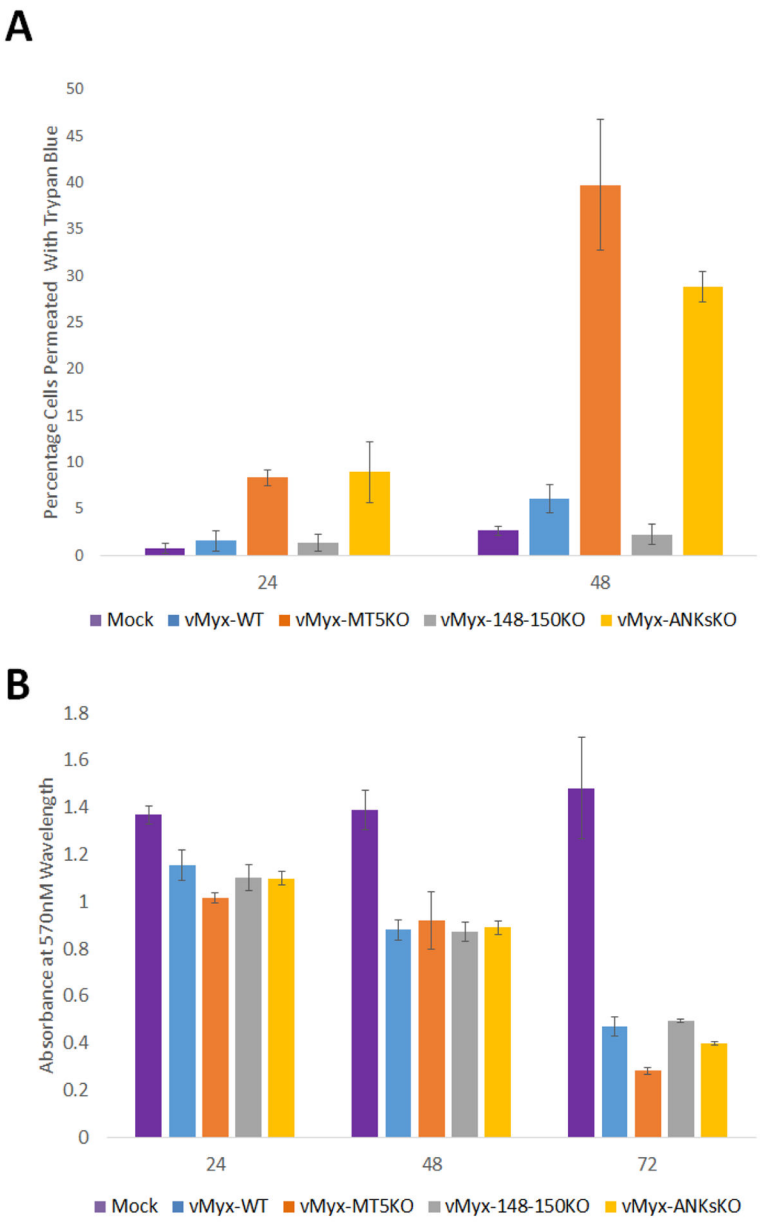

Figure 5. Detection of cytotoxicity following infection with ANK-R mutant myxoma viruses

A) A549 cells were mock infected or infected with vMyx-WT, vMyx-MT5KO, vMyx-148–150KO, or vMyx-ANKsKO viruses and cell membrane integrity, as a surrogate for cell death, was detected by trypan blue exclusion assay. Values are expressed as the mean percentage of trypan blue-positive cells (± standard deviation [SD]) from triplicate experiments. B) Cell viability as assessed by mitochondrial function levels following infection was measured by MTT assay. Results are displayed as mean absorbance (± standard deviation [SD]) from triplicate experiments.

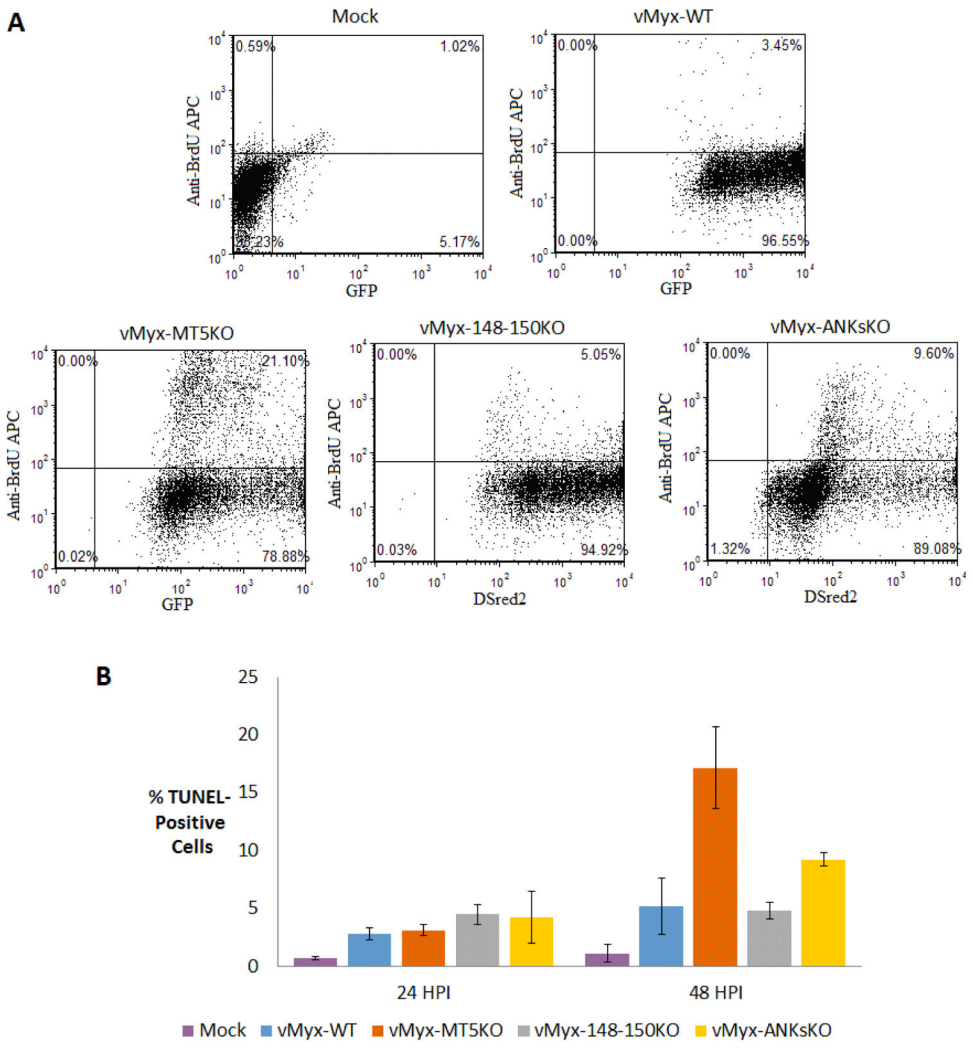

Figure 6.

DNA fragmentation analysis of A549 cells following infection with ANK-R mutant myxoma viruses. Fragmented DNA in ANK-R mutant myxoma virus infected cells was labeled with BrdU and used as a marker for apoptosis. A) A graphical representation of anti-BrdU APC labeled cells (10,000 events) at 48 hours post mock infection or infection with vMyx-WT (GFP), vMyx-MT5KO (GFP), vMyx-148–150KO (DSred2), and vMyx-ANKsKO (DSred2). B) The mean percentage of TUNEL-positive cells (± standard deviation [SD]) from triplicate experiments at both 24 and 48 HPI with ANK-R mutant myxoma viruses.

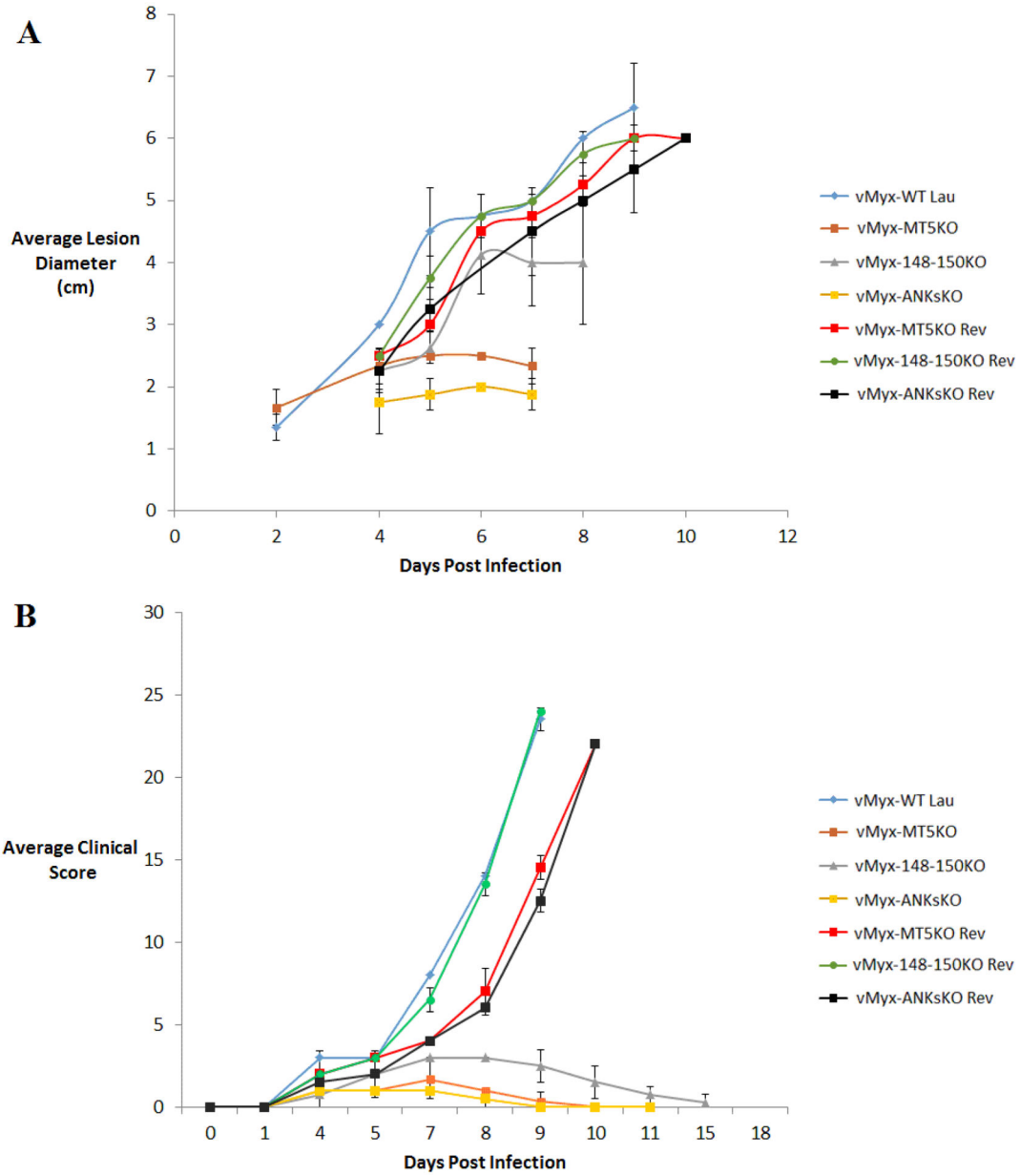

Figure 7. Attenuation of myxoma virus virulence during ANK-R mutant infection of rabbits

NZW rabbits were inoculated intradermally with 1000 FFU of vMyx-WT (n=2), vMyx-MT5KO (n=3), vMyx-148–150KO (n=4), vMyx-ANKsKO (n=4) and the various revertant MYXVs (n=3 each). A) Calipers were used to measure primary lesion diameter throughout the course of virus infection. Values are expressed as the mean lesion diameter (± standard deviation [SD]). Lesions with exceptionally small diameters, eg. during initial growth or late recovery, were excluded from this chart. B) After daily physical examinations, clinical scores for infected rabbits were calculated based on abnormal respiration, weight, temperature, heart rate, lung sounds, food and water intake, urine and feces output,

hydration status, attitude, posture, indications of primary lesion and appearance of secondary lesions. Values are expressed as the mean clinical score (± standard deviation [SD]).

Table 1

Nomenclature and characteristics of ANK-R knockout myxoma viruses

Virus Name	Abbreviation	Genetic Alterations
vMyx-WT Lausanne	vMyx-WT Lau	N/A
vMyx-WT LacZ GFP	vMyx-WT	Intergenic p11 LacZ between *M010* and *M011* Intergenic EL GFP between *M135* and *M136*
vMyx-MT5KO LacZ GFP Eco GPT	vMyx-MT5KO	Intergenic p11 LacZ between *M010* and *M011* Intergenic EL GFP between *M135* and *M136* Intragenic EL Eco GPT within *M-T5*
vMyx-M148/M149/150KO DSred2	vMyx-148–150KO	EL DSred2 replacing *M148–M150*
vMyx-MT5KO/M148/M149/M150KO LacZ Eco GPT DSred2	vMyx-ANKsKO	Intergenic p11 LacZ between *M010* and *M011* Intragenic EL Eco GPT within *M-T5* EL DSred2 replacing *M148–M150*
vMyx-MT5KO Revertant	vMyx-MT5KO Rev	Intergenic EL GFP between *M135* and *M136* Intergenic p11 LacZ between *M010* and *M011*
vMyx-M148/M149/150KO Revertant	vMyx-148–150 KO Rev	N/A
vMyx-MT5KO/M148/M149/M150-KO Revertant	vMyx-ANKsKO Rev	Intergenic EL GFP between *M135* and *M136* Intergenic p11 LacZ between *M010* and *M011*

EL- Vaccinia Virus synthetic early/late promoter p7.5

P11- Vaccinia Virus late promoter

Table 2

Primer sequences used to create and genotype recombinant myxoma virus

Primer Name	Sequence
attB1_F	GGGGACAAGTTTGTACAAAAAAGCAGGCTCCACC
attB2_R	GGGGACCACTTTGTACAAGAAAGCTGGGTCCAA
1_attB1M147F	AAAGCAGGCTCCACCACCAGTGTTTTATACACAAAGGAG
2_5M148ELF	GGATTATCTAAAGAAAGAACTCTGCAGGTCGACTCTAG
3_RED3M150R	CGATGGCTTGAATGTTAGAATTCGAGCTCGGTAC
4_M151R	ACAAGAAAGCTGGGTCCAAGCTGTCGTACCGAACTCGGTC
attB1_MT5F	AAAGCAGGCTCCACCCTCGATAATCGCGAGTACATTTTC
attB2_MT5R	ACAAGAAAGCTGGGTCCAAGATTCCGGACGTGGAATATTGGAC
M147_F_full_attB1	GGGGACAAGTTTGTACAAAAAAGCAGGCTCCACCACCAGTGTTTTATACACAAAGGAG
M151_R_full_attB2	GGGGACCACTTTGTACAAGAAAGCTGGGTCCAAGCTGTCGTACCGAACTCGGTC
M149GenotypingF	AGACGTCCGGGTAGAACGTTGA
M149GenotypingR	TGTGGAACTCCGGACACACGGT
M147GenotypingF	ACAACGCGACAACTGCCGAC
M151GenotypingR	TGCCCTCGTTCCTCACGTCCA
MT5GenotypingF	TGTCGTGTACGCCTCGTATC
MT5GenotypingR	TTGAACCGTCGCTTGTGTAG

Table 3

Criteria for Scoring Virus-Infected Rabbits

Assessments	Points			
	0	1	2	4
Posture	**Normal** Sitting erect, ears up, moving freely, lying stretched out	**Abnormal** Some reduction in spontaneous activity, will move with gentle encouragement but prefers to be inactive. Change in posture.	**Very Abnormal** Little to no spontaneous activity.	
Eating and Drinking	**Normal**		**Abnormal** Reduced intake	**Very Abnormal** Minimal intake
Attitude	**Normal** Bright and alert, interested in surroundings; usual temperament	**Abnormal** A bit dull but still active in investigating new situation, objects placed in pen.	**Very Abnormal** Very dull, not interested in surroundings, preoccupied.	
Hydration	**Normal** No tent or twist	**Abnormal** Tent, but returns to shape after <30 seconds	**Very Abnormal** Tent and does not return to shape readily	
Eyes	**Normal**	**Abnormal** Conjunctivitis either unilateral or bilateral. May have occasional nodules. Eyes are not closed.	**Very Abnormal** Severe conjunctivitis with purulent discharge. Eyes may be partially closed. Lids swollen	
Nose	**Normal**	**Abnormal** Some swelling or discharge either purulent or purulohaemorrhagic.	**Very Abnormal** Severe swelling and/or profuse discharge	
Respiration	**Normal**		**Abnormal** >10% difference from daily average in uninfected	**Very Abnormal** >20% difference from daily average in uninfected
Ears	**Normal**	**Abnormal** Some swelling or discharge either purulent or purulohaemorrhagic	**Very Abnormal** Severe swelling and/or profuse discharge	
Heart Rate	**Normal** 180–250 bpm	**Abnormal** 140–180 bpm	**Very Abnormal** <140 bpm	
Temperature	**Normal** 101.3–104°F	**Abnormal** 104.1–106°F	**Very Abnormal** >106°F	
Weight	**Normal** Constant weight gain	**Abnormal** No weight gain	**Very Abnormal** Weight loss	
Feces	**Normal** Normal amount and consistency	**Abnormal** Reduced amount or alteration in consistency	**Very Abnormal** Minimal elimination or very liquid feces	
Injection site	**Normal** No swelling/reaction at site	**Abnormal** Ulceration and/or diffuse reaction	**Very Abnormal** Severe swelling of lesion, necrosis, etc.	
Viremia (secondary lesions other than nose, ear and eye)	**Normal** No secondary lesions present.		**Abnormal** Secondary lesions present, minimal	**Very Abnormal** Secondary lesions present, severe.

Conditions which require immediate euthanasia

If a rabbit reaches a score of 26/34, or should it exhibit any of the following conditions, it will be euthanized immediately:

1. Orthopnea
2. Mouth breathing
3. Cyanosis

4. Essentially no food or water intake >48 hrs

Table 4

Pathogenesis of ANK-R MYXV constructs in New Zealand White (NZW) rabbits

Day	vMyx-WT and Revertants	vMyx-MT5KO	vMyx-148–150KO	vMyx-ANKsKO
0	Inoculation of two rabbits intradermally with 1,000 PFU or FFU for each of the following viruses: vMyx-WT Lausanne, vMyx-MT5KO Revertant, vMyx 148–150 Revertant, vMyx-ANKsKO Revertant	Inoculation of three rabbits intradermally with 1,000 FFU of vMyx-MT5KO	Inoculation of four rabbits intradermally with 1,000 FFU of vMyx-148–150KO	Inoculation of four rabbits intradermally with 1,000 FFU of vMyx-ANKsKO
4	Primary lesions at inoculation sites: 2.0–3.0 cm (8/8) Raised, soft, red lesions (4/8) Raised, red, necrotic lesions (4/8) Multiple secondary lesions on ears (5/8)	Primary lesions at inoculation sites: Raised, soft, red (ca 2.0–2.5 cm) (3/3)	Primary lesions at inoculation sites: Raised, soft, red (ca 2.0–2.5 cm) (4/4) One rabbit exhibited minute secondary lesions on the ear	Primary lesions at inoculation sites: Raised, soft, red (ca. 1.5–2.5 cm) (4/4)
7	Primary lesions red, swollen, necrotic (4.0–5.0 cm) 8/8 Multiple secondary myxomas in the eyes, ears, and nose. (8/8) Gram-negative bacteria infections of conjunctivas (7/8)	Primary lesions red, swollen, necrotic, healing (2.0–2.5 cm) (3/3)	Primary lesions red, swollen, necrotic (ca 3.5–5.0 cm) (4/4) Multiple minute secondary myxomas (4/4), gram-negative bacterial infections of conjunctivas (2/4)	Primary lesions red, swollen, necrotic (ca. 1.5–2.0 cm) (4/4)
9–10	Primary lesions red, swollen, necrotic (5.0–6.0 cm) (8/8) Multiple secondary myxomas, turning necrotic, dyspnea, severe infections of respiratory tracts, prostrated and emaciated animals. All rabbits were sacrificed due to the severity of symptoms	Primary lesions swollen, but healing	Primary lesions swollen, but healing Secondary lesions healing (4/4)	Primary lesions swollen, but healing
17		Full regression of primary lesions	Full regression of primary and secondary lesions	Full regression of primary lesions